



HAL
open science

Microstructure, indentation and work hardening of Cu/Ag multilayers

Marc Verdier, H. Huang, Frans Spaepen, J. David Embury, Harriet Kung

► **To cite this version:**

Marc Verdier, H. Huang, Frans Spaepen, J. David Embury, Harriet Kung. Microstructure, indentation and work hardening of Cu/Ag multilayers. *Philosophical Magazine*, 2006, 86 (32), pp.5009-5016. 10.1080/14786430600746440 . hal-00513707

HAL Id: hal-00513707

<https://hal.science/hal-00513707>

Submitted on 1 Sep 2010

HAL is a multi-disciplinary open access archive for the deposit and dissemination of scientific research documents, whether they are published or not. The documents may come from teaching and research institutions in France or abroad, or from public or private research centers.

L'archive ouverte pluridisciplinaire **HAL**, est destinée au dépôt et à la diffusion de documents scientifiques de niveau recherche, publiés ou non, émanant des établissements d'enseignement et de recherche français ou étrangers, des laboratoires publics ou privés.



Microstructure, indentation and work hardening of Cu/Ag multilayers

Journal:	<i>Philosophical Magazine & Philosophical Magazine Letters</i>
Manuscript ID:	TPHM-06-Jan-0018.R1
Journal Selection:	Philosophical Magazine
Date Submitted by the Author:	29-Mar-2006
Complete List of Authors:	Verdier, Marc; ENSEEG, LTPCM Huang, H.; Harvard University, Division of Engineering and Applied Sciences Spaepen, Frans; Harvard university, Div. of Eng. and Applied Sciences Embury, J. David; McMaster University, Materials Science and Engineering Kung, Harriet; Los Alamos National Laboratory
Keywords:	multilayers, nanomaterials, plasticity of metals
Keywords (user supplied):	



Microstructure, indentation and work hardening of Cu/Ag multilayers

M. Verdier^{(1)†}, H. Huang^{(2)*}, F. Spaepen⁽²⁾, J.D. Embury⁽¹⁾, H. Kung⁽¹⁾

(1) Los Alamos National Laboratory, CMS, Mail Stop K765, Los Alamos, NM 87544

(2) Division of Engineering and Applied Sciences, Harvard University, Cambridge MA 02138

† Present address (corresponding author):

LTPCM (CNRS UMR 29), Domaine Universitaire, BP75 38402 S^t Martin d'Hères Cedex, France

mverdier@ltpcm.inpg.fr

fax: (33) 4 76 82 66 44

Manuscript : 2380 words

Microstructure, indentation and work hardening of Cu/Ag multilayers

M. VERDIER^{(1)†}, H. HUANG^{(2)*}, F. SPAEPEN⁽²⁾, J.D. EMBURY⁽¹⁾, H. KUNG⁽¹⁾

(1) Los Alamos National Laboratory, CMS, Mail Stop K765, Los Alamos, NM 87544

(2) Division of Engineering and Applied Sciences, Harvard University, Cambridge MA 02138

† Present address: LTPCM (CNRS UMR 29), Domaine Universitaire, BP75 38402 S^t Martin d'Hères Cedex, France

* Present address: General Atomic, Internal fusion technology division, San Diego, CA

Abstract

Instrumented indentation and tensile tests were performed on free standing Cu/Ag multilayer thin films with layer thicknesses in the range 0.85-900 nm. The effect of layer thickness can be described by a Hall-Petch relationship. The work hardening rate in the tensile test depends on layer thickness which indicates that the interfaces create storage sites for dislocations and follows an inverse power law.

Keywords: plasticity in metals, nanomaterials, multilayers

Introduction:

The interest in the mechanical properties of metallic multilayers reflects both the importance of their technological applications and the need to understand the influence of the length scale on a variety of fundamental deformation processes [1]. One important question is the sequence of plastic yielding, work hardening and fracture in fine scale lamellar structures. This topic has relatively few detailed

1
2
3 experimental studies. The problem of characterizing fine scale structures is complex because the
4
5 microstructure depends on the processing route, the nature of substrate, the level of contamination, the
6
7 level of residual stress, etc., all of which can influence the mechanical response. The current work
8
9 concerns the mechanical behavior of thin films of Cu, Ag, and multilayers of Cu/Ag prepared by
10
11 physical vapor deposition (PVD) at room temperature. The residual stresses and tensile behavior of
12
13 these materials have been reported in earlier papers [2],[3]. In this paper we report additional
14
15 mechanical tests (depth sensing indentation), a more detailed analysis of the relation between the
16
17 mechanical behavior and the microstructural characteristics, and an analysis of the work hardening.
18
19
20
21
22
23
24
25
26

27 **Materials and Experiments**

28
29
30
31
32 The plastic deformation of the two fcc metals chosen for this study, Cu and Ag, has been thoroughly
33
34 studied in their pure bulk form. Their limited mutual solubility at room temperature results in sharp
35
36 compositional interfaces in the multilayer structure. The lattice misfit between the two phases is large
37
38 (10.5%), as is the ratio of the elastic moduli (for example for the shear moduli, $G_{Cu}/G_{Ag} \approx 1.5$ [4]). Both
39
40 properties, through the presence of misfit dislocations and image forces, influence the yield behaviour.
41
42 The Cu, Ag and Cu/Ag films were deposited by electron beam evaporation on glass substrates at room
43
44 temperature (base pressure: 10^{-7} torr; deposition rate 0.2-1 nm/s) The glass substrate allows easy
45
46 removal of the film. The films (pure metals and multilayers) have a thickness around 2 μm and the
47
48 range of layer thicknesses (h) in the multilayers varies between 1000 nm (bilayers) to 0.85 nm (several
49
50 thousands of layers).
51
52
53
54
55
56
57
58
59
60

1
2
3 The microstructure of the films was characterized by cross-sectional transmission electron microscopy
4 (TEM) using a Philips CM30 (300kV), the surfaces were observed by atomic force microscopy (AFM)
5 in tapping mode (Digital Instruments 3100) and X-ray diffraction is done using a standard θ -2 θ
6 diffractometer. Free-standing films were tested in tension using optical diffraction for the strain
7 measurement [2],[5]. The strain rate used in the tests was 10^{-4} s^{-1} . Multilayers with small layer
8 thickness (0.85-190 nm) were tested on their substrate by nanoindentation, using a Nanoindenter II with
9 a Berkovich tip, and with the Continuous Stiffness Measurement module which allows determination
10 of the area of contact at any indentation depth. The standard Oliver-Pharr procedure was used to
11 determine both the hardness and the Young modulus of the films [6].
12
13
14
15
16
17
18
19
20
21
22
23
24
25
26
27
28
29

30 Results

31 A) *microstructure*

32
33
34
35 Cross-sectional TEM images of the multilayers are shown in Figure 1. Columnar grains along the
36 growth direction are clearly visible, with an average column diameter on the order of 100-150 nm. The
37 foils have undergone less than 0.3% total tensile strain. Figure 1(b) shows the microstructure of the
38 individual layers, and the waviness of the interfaces. This is related to the island growth during
39 deposition at room temperature which gives rise to the columnar grain structure [7]. The selected area
40 diffraction pattern shows a strong texture ($\langle 111 \rangle$) along the growth direction of the film.
41
42 Crystallographic orientations with (111) planes parallel to the plane of the film are expected for fcc
43 metals deposited at room temperature on lower surface energy substrates such as the glass used in this
44 work [8].
45
46
47
48
49
50
51
52
53
54
55
56
57
58
59
60

[Insert Fig 1]

The layers consist of grains or subgrains with diameter around 100 nm. Strong strain contrast did not permit the imaging of single dislocations within the grains. No voids were observed in the foils using defocus conditions and the macroscopic density, measured by a combination of weighing and thickness measurements with a profilometer, is within 1% of the theoretical value.

B) Mechanical properties

The stress-strain curves for the pure Cu and Ag films, and for the different multilayers are shown in figure 2. The data are the outer envelopes of the loading-unloading data reported in [2]. In the multilayers, the 0.2% yield stress increases with decreasing layer thickness, h , according to a Hall-Petch type relationship:

$$\sigma_{0.2} = \sigma_0 + kh^{-0.5} \quad (1)$$

where h is the layer thickness and σ_0 and k are constants ($\sigma_0 = 223 \pm 16$ MPa, $k = 0.104 \pm 0.01$) [2].

[Insert Fig. 2 here]

In the finest structures ($h < 160$ nm) the 0.2% yield stress could not be measured because fracture intervened. The increase in both yield stress and work hardening, combined with increased fragility of the films with the finest layers, limited the amount of plastic strain that could be achieved. Therefore to extend the range of measurements to finer structures, nanoindentation measurements were performed on some films still attached to their glass substrates, for layer thicknesses between 190 and 0.85 nm.

1
2
3 Figure 3 shows the effective Young's modulus and the hardness as a function of indentation depth. The
4 glass substrates have a lower modulus than the films (70 GPa), so that a continuous evolution with
5 indentation depth from the film values to the substrate values is observed. The Young moduli of the
6 multilayers as measured in tensile tests or in instrumented indentation are in the same range, ie between
7 85 and 95 GPa. The indentation depths are normalized with respect to the film thicknesses. The
8 resulting value, the relative depth, is used for comparisons.
9
10
11
12
13
14
15
16
17
18
19

20 [Insert Fig 3 here]
21
22
23
24

25 The hardness values at a relative depth of 10% are plotted in Figure 4 together with the data obtained
26 from tensile experiments using the Tabor relation between hardness and yield stress ($H= 3\sigma$).
27
28
29
30
31

32 [Insert Fig.4 here]
33
34
35
36

37 The same dependence on the layer thickness is observed in both sets of data, but the values derived
38 from hardness tests are higher. This difference may be due to several factors. First, due to the
39 indentation size effect [9] there is a decrease of the measured hardness, by about a factor of two. To
40 compare the data from films of different thicknesses, we used the initial plateau value of the curves
41 $H(\text{relative depth})$ which is reached for a relative depth of 10%. Finally, work hardening plays a very
42 important role. The average plastic strain in an indentation experiment is equivalent to 7% in elasto-
43 pure plastic materials [10]. Since the initial work hardening in the films is very high, especially for the
44 smallest layer thicknesses, the flow stress measured by indentation is substantially greater than the
45 0.2% yield stress.
46
47
48
49
50
51
52
53
54
55
56
57
58
59
60

1
2
3 It is clear, however, that the increase in flow stress of these laminates with decreasing layer thickness
4 indicates that no softening at small layer thickness occurs for Cu/Ag, unlike in other fcc/fcc multilayers
5
6 such as Cu/Ni [11].
7
8
9

10
11
12
13 The work hardening behaviour can be analyzed using a plot (Figure 5) of the plastic work hardening
14 rate, $\theta = d\sigma/d\varepsilon_{\text{plastic}}$, versus the stress σ , calculated from the tensile stress-strain curves of figure 2.
15
16
17

18
19
20 [Insert Fig. 5 here]
21
22
23
24

25 We do not consider the stress-strain curves of multilayers with layer thickness less than 46 nm, since
26 fracture occurs at the onset of plasticity. In a bulk material, an average value of the theoretical
27 maximum work hardening reached during tensile straining by a single crystal, i.e. during stage II of
28 plastic deformation $((d\tau/\gamma)_{\text{II}})$ where τ, γ are respectively the resolved shear stress and strain can be
29 estimated. For a polycrystalline material this can be approximated by [16]:
30
31
32
33
34
35

$$\langle \theta_{\text{II}} \rangle = d\sigma/d\varepsilon = M^2 (d\tau/\gamma)_{\text{II}} = M^2 \langle G_{\text{Cu,Ag}} \rangle / 200 = 1665 \text{ GPa}, \quad (2)$$

36
37
38 where $M=3$ (Taylor factor), and $\langle G_{\text{Cu,Ag}} \rangle$ is the arithmetic average of the Voigt averages $G_{\text{Cu}}=48 \text{ GPa}$,
39
40
41 $G_{\text{Ag}}=27 \text{ GPa}$ [4]
42
43

44 The initial work hardening rates observed in these thin films are initially higher than θ_{II} . Possible
45 reasons for this are discussed below.
46
47
48
49
50
51

52 Discussion

53
54 The scale of the multilayers clearly influences both the initial yield strength and the rate of work
55 hardening. There are two possible length scales that can influence the mechanical response, the
56
57
58
59
60

diameter of the columnar structure and the layer spacing. The columnar structure remains essentially constant as the layer spacing decreases. It appears that the length scale controlling both yielding and work hardening is the layer spacing h .

Using the formalism developed by Kocks [15],[16] for the evolution of dislocation density, ρ , the model can be modified so that not only dislocation/dislocation interactions are taken into account through their average separation distance ($L=\rho^{-1/2}$), but another set of obstacles with spacing h is also included. We assume that both storage mechanisms act in parallel, so that the effective inverse obstacle spacing becomes $1/L+1/h$. The evolution of the dislocation density can be written following previous work in [14-16]:

$$\frac{d\rho}{d\varepsilon} = M(k_1\sqrt{\rho} + k_2 - k_3\rho) \quad (3)$$

with the k_i constant during the test; $k_3 = k_2 + K/h$, with K a constant, is the efficiency to recover dynamically at the obstacles of spacing h [14]. Since

$$\sigma = M\alpha G b \rho^{1/2}, \quad (4)$$

with α constant ($\alpha \approx 0.3$ for Cu [17]), $\theta(\sigma) = d\sigma/d\varepsilon$ can be written as

$$\theta(\sigma) = \theta_{II} + \frac{P_1}{\sigma} - P_2 \sigma \quad (5)$$

with

$$P_1 = M^3 (\alpha G)^2 \frac{b}{2h}, \quad (6)$$

and

$$P_2 = \frac{\theta_{II}}{\sigma_{sat}} + \frac{KM}{2h} \quad (7)$$

where σ_{sat} is the saturation stress of the single crystal [11]. The accumulation P_2 term contains both storage from dislocation interactions (θ_{II} –forest model) as in the bulk single crystal and storage at the interface ($1/h$ term). In the following we will focus on P_1 term which can be expressed in terms of

1
2
3 physically based parameter. The values of P_1 are obtained by fitting equation (5) to the experimental
4
5 curves of figure 5b. Figure 6 shows a comparison of the obtained values of P_1 with the prediction given
6
7 by equation (6). It can first be observed in figure 6 that the slope between $\log(P_1)$ and $(1/h)$ is close to
8
9 unity which shows the importance of the layer spacing on the storage term of the work hardening.
10
11 Secondly considering the simplifying assumptions made (isotropic elasticity, average values of shear
12
13 moduli, theoretical value of stage II), the values are in good agreement with the simplified model.
14
15 Moreover we observe at large length scale a nearly constant value: this can be due to the internal
16
17 microstructure of columnar grains, i.e. the layer period turns to be larger than the columnar grain size.
18
19 Thus for large layer thickness (greater than 600nm) the geometrical work hardening storage term seems
20
21 to be controlled not by the layer spacing but by the structural grain size within the layers.
22
23
24
25
26
27
28
29

30 [Insert Fig.6 here]
31
32
33
34

35 Conclusion

36
37 The depth sensing indentation experiments on the Cu/Ag multilayers have shown that the Hall-Petch
38
39 relation between yield stress and layer thickness extends to the smallest layer thicknesses. No evidence
40
41 of any softening was found. The initial work hardening rate in the tensile experiments is higher than the
42
43 maxima observed for bulk single crystal. This implies the presence of an additional set of obstacles to
44
45 the dislocation motion. Based on a simplified model of the evolution of dislocation density, we observe
46
47 a linear relationship between the initial work hardening parameter and the inverse of the layer spacing.
48
49
50
51
52
53
54
55
56
57
58
59
60

Acknowledgments

Los Alamos Nat Lab. and NSERC Canada are acknowledged for financial support. The work at Harvard was supported by the Harvard Materials Research Science and Engineering Center under Contract number DMR 98-09363. H.H. acknowledges support from an AlliedSignal predoctoral fellowship.

For Peer Review Only

References

- [1] H. Kung, T. Foecke guest eds., Mechanical behavior of nanostructures materials, MRS Bulletin, **24** (2) (1999)
- [2] H. Huang and F. Spaepen, *Acta Mat.* **48**, 3261 (2000)
- [3] A.L. Shull and F. Spaepen, *J. Appl. Phys.* **80**, 6243 (1996)
- [4] Single crystal elastic constants and calculated aggregate properties: a handbook, G. Simmons, H. Wang, M.I.T Press (1971)
- [5] J.A. Ruud, D. Josell, F. Spaepen, A.L. Greer, *J. Mat. Res.* **8**, p 112 (1993).
- [6] W.C. Oliver, G.M. Pharr, *J. Mat. Res.*, **7**, 1564 (1992)
- [7] C.R.M. Grovenor, H.T.G. Hentzell, D.A.Smith, *Acta Metall.* , **32**, p 773 (1984)
- [8] C.V. Thompson, *Annu. Rev. Mater. Sci.* 2000. 30:159–90
- [9] W.D. Nix, *Mat. Sci. and Eng. A*, **234-236** pp37-44 (1997)
- [10] K.L. Johnson, *Contact Mechanics*, Cambridge Uni. Press (1985)
- [11] M. Verdier, M. Niewczas, J. D. Embury, M. Hawley, M. Nastasi and H. Kung ,MRS Proc., **522** p77-82 (1998)
- [12] J.D. Embury, J.P. Hirth, *Acta Met. et Mat.* **42**(6) pp 2051-2056 (1994)
- [13] W.D. Nix, *Scripta Mat.*, **39** (4/5), pp 545-554 (1998)
- [14] M. Verdier, Y. Bréchet, P. Guyot, *Acta Mat.*, **47**, p127 (1998)
- [15] Y. Estrin, Unified Constitutive laws of plastic deformation, Ed. Krausz and Krausz, Academic Press (1996)
- [16] U.F. Kocks, H.Mecking, *Prog. In Mat. Science*, **48**, pp171-273 (2003)

1
2
3 [17] S.J. Basinski, Z.S. Basinski, Dislocations in solids, 4, pp. 260, F.R.N. Nabarro Ed., Amsterdam
4
5
6 North Holland (1979).
7
8
9
10
11
12
13
14
15
16
17
18
19
20
21
22
23
24
25
26
27
28
29
30
31
32
33
34
35
36
37
38
39
40
41
42
43
44
45
46
47
48
49
50
51
52
53
54
55
56
57
58
59
60

For Peer Review Only

Figure captions:

Figure 1: (a)-(b) Cross-sectional TEM images of a multilayer after tensile deformation; the layer thickness is 200Å. In (b) the corresponding diffraction pattern is inserted and (111) reflections are indicated.

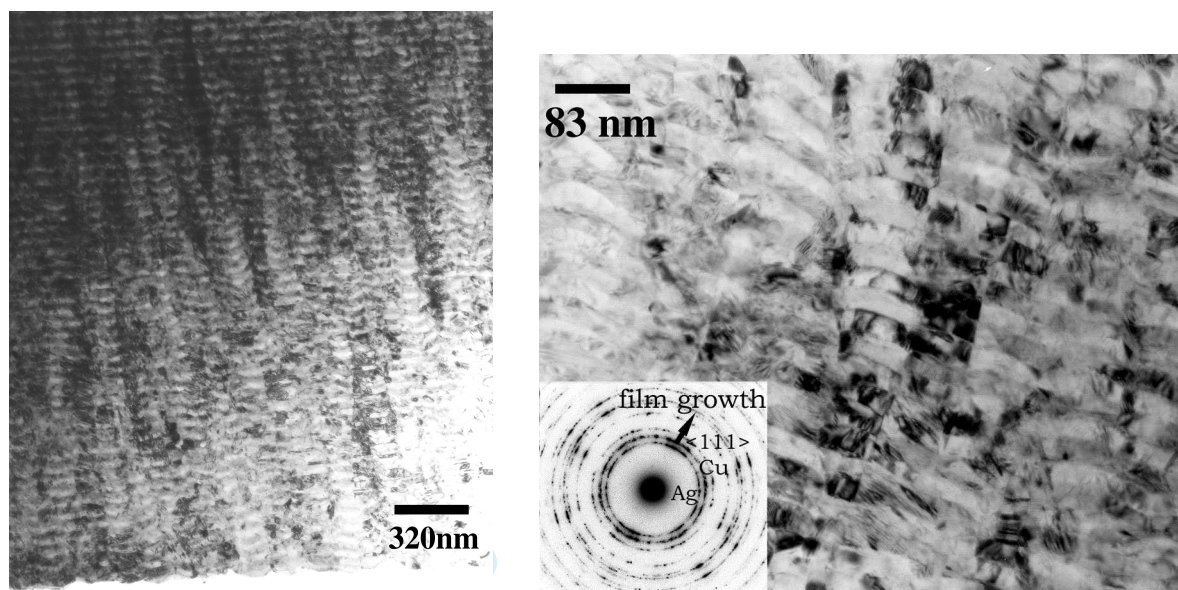
Figure 2 - Stress-strain curves in tensile testing of (a) free standing pure thin films of Cu and Ag, and (b) Cu/Ag multilayers with different layer thicknesses (total thickness around 2.5µm). Adapted from ref. [1].

Figure 3 - Dependence of the effective Young modulus (E) and hardness (H) on the relative indentation depth for multilayers with various layer thicknesses.

Figure 4 Comparison of 0.2% yield stress from tensile tests and hardness from nanoindentation.

Figure 5: (a) True plastic stress-strain curves and (b) Work hardening versus stress deduced from Figure 2 (b) . A constant Young modulus of 91GPa is used. In figure 2b, the line indicates the Considère instability limit (onset of striction).

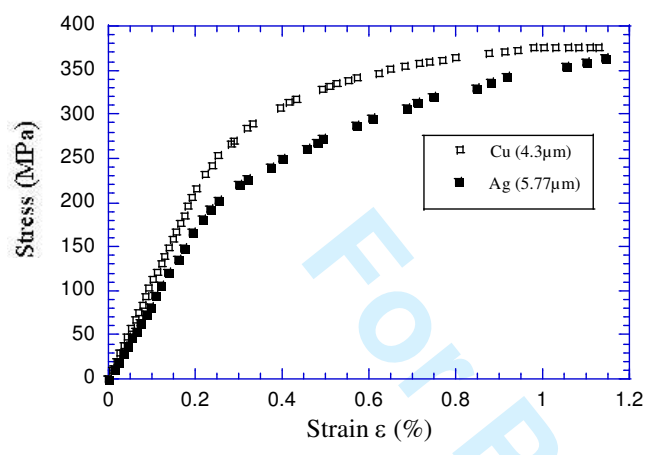
Figure 6: Experimental and model value of storage term P1 versus the inverse layer thickness



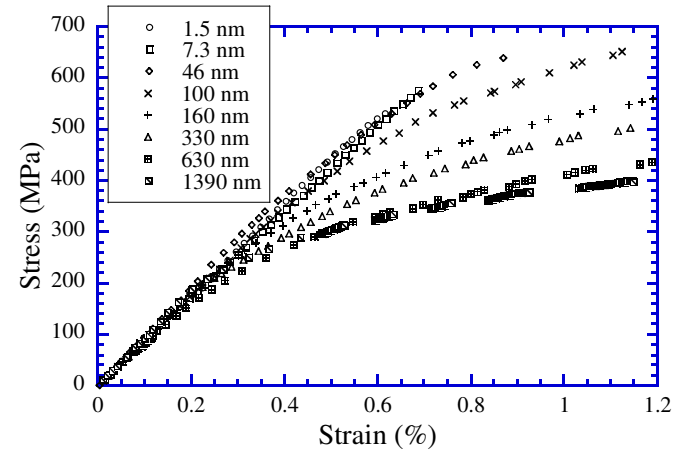
(a)

(b)

Fig1

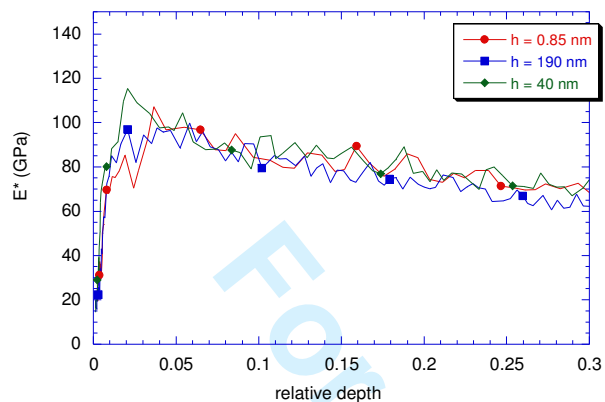


(a)

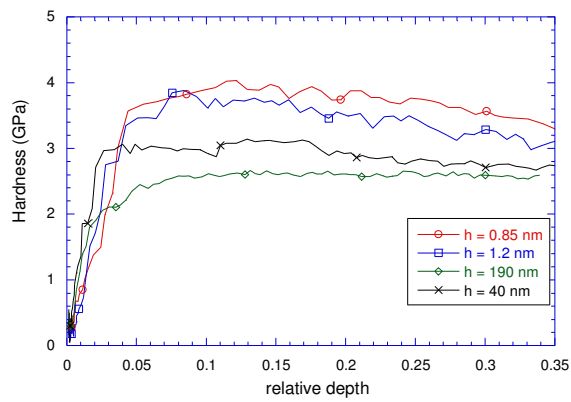


(b)

Fig. 2



(a)



(b)

Fig.3

1
2
3
4
5
6
7
8
9
10
11
12
13
14
15
16
17
18
19
20
21
22
23
24
25
26
27
28
29
30
31
32
33
34
35
36
37
38
39
40
41
42
43
44
45
46
47
48
49
50
51
52
53
54
55
56
57
58
59
60

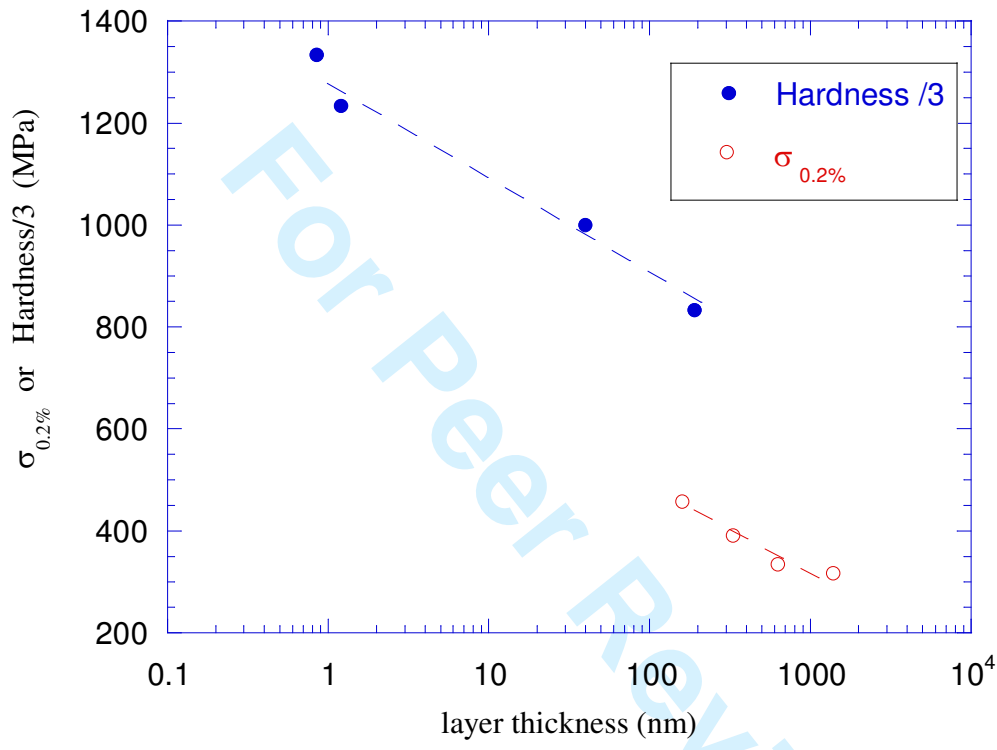
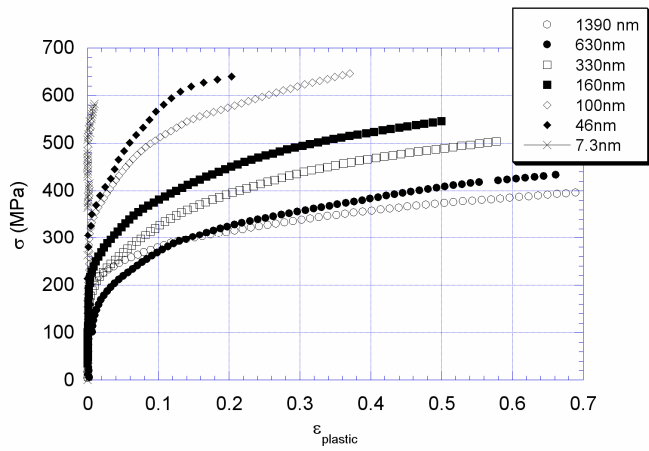
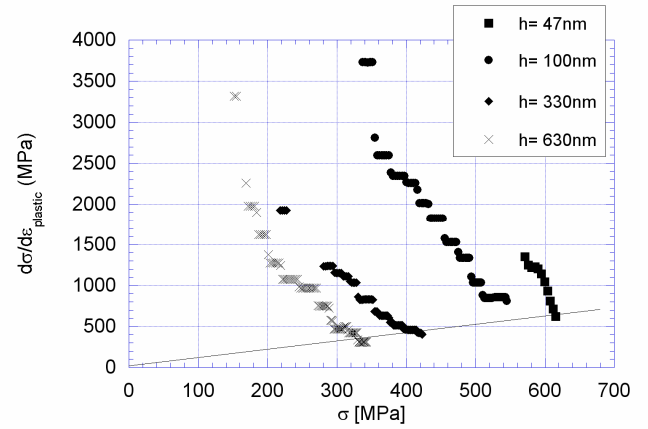


Fig. 4



(a)



(b)

Fig. 5

1
2
3
4
5
6
7
8
9
10
11
12
13
14
15
16
17
18
19
20
21
22
23
24
25
26
27
28
29
30
31
32
33
34
35
36
37
38
39
40
41
42
43
44
45
46
47
48
49
50
51
52
53
54
55
56
57
58
59
60

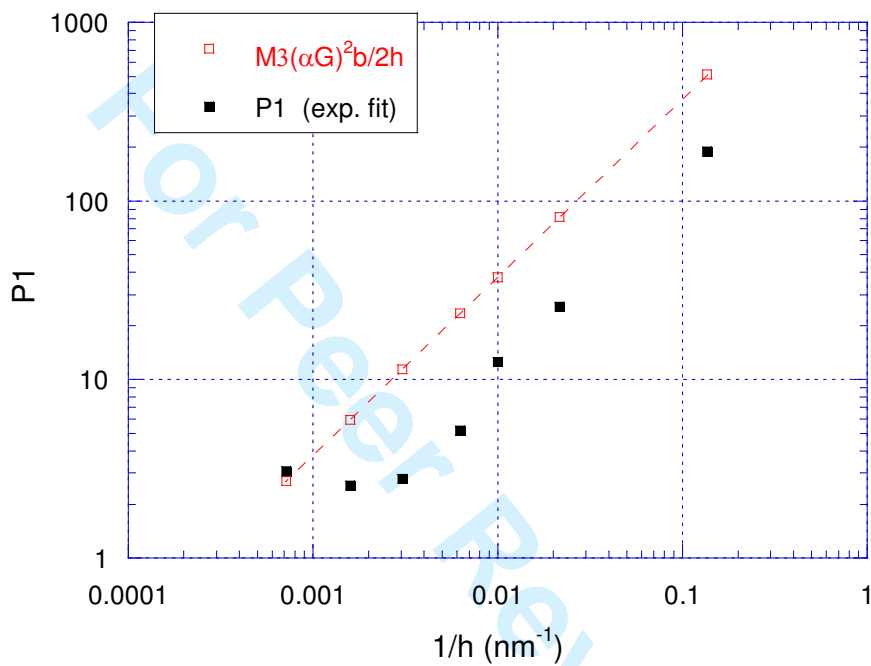
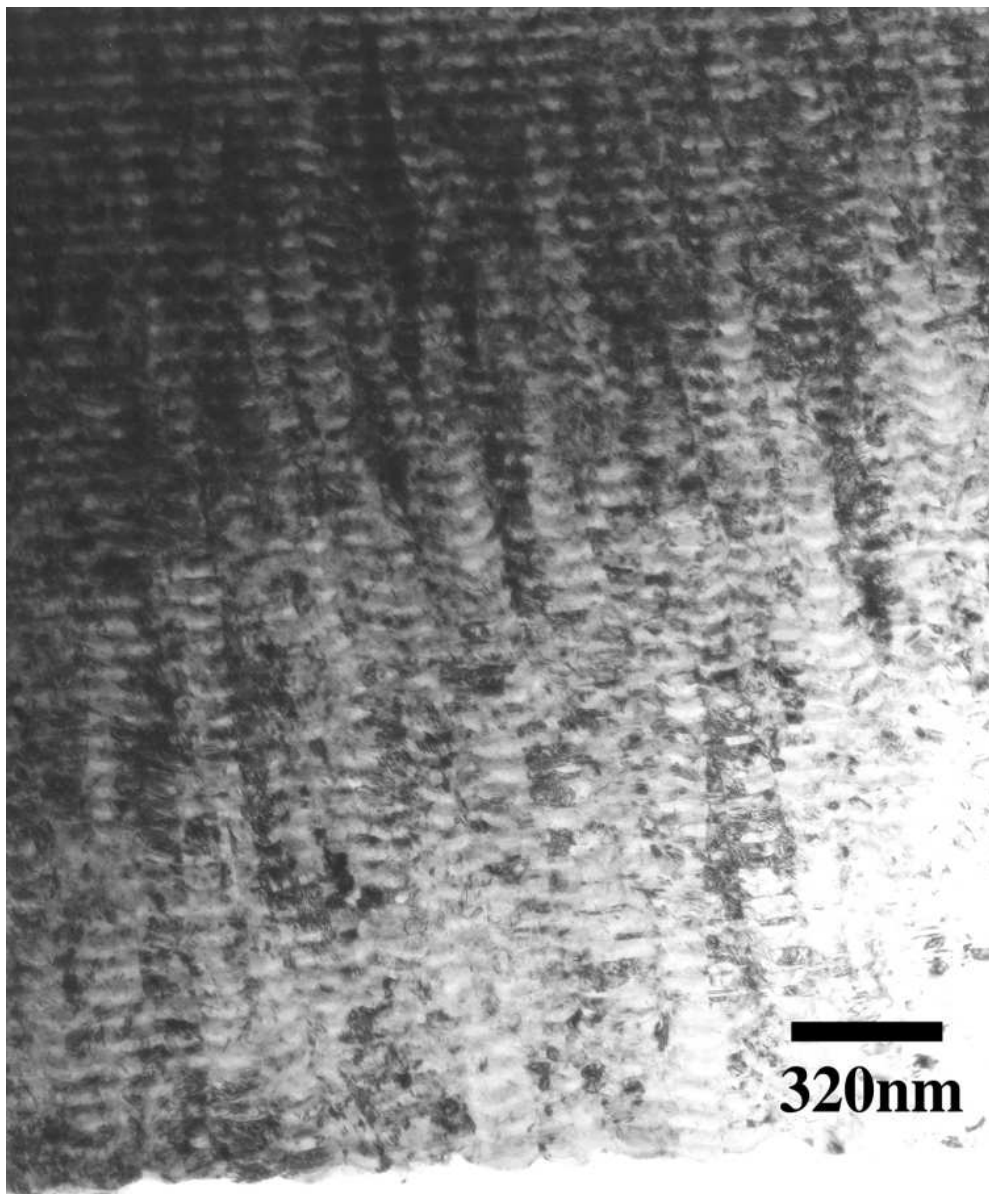


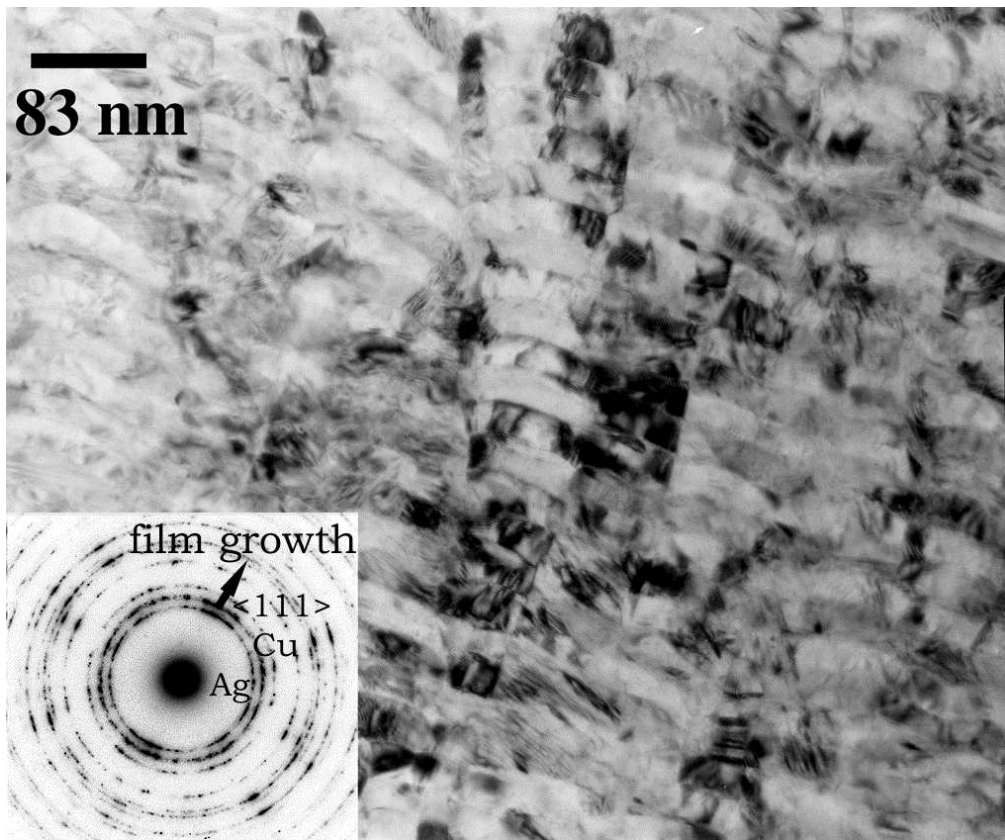
Fig 6

1
2
3
4
5
6
7
8
9
10
11
12
13
14
15
16
17
18
19
20
21
22
23
24
25
26
27
28
29
30
31
32
33
34
35
36
37
38
39
40
41
42
43
44
45
46
47
48
49
50
51
52
53
54
55
56
57
58
59
60



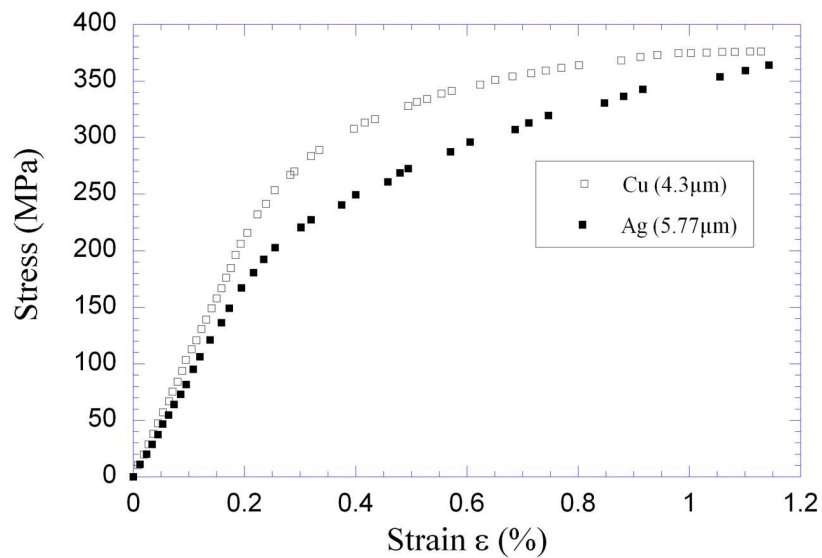
63x77mm (300 x 300 DPI)

1
2
3
4
5
6
7
8
9
10
11
12
13
14
15
16
17
18
19
20
21
22
23
24
25
26
27
28
29
30
31
32
33
34
35
36
37
38
39
40
41
42
43
44
45
46
47
48
49
50
51
52
53
54
55
56
57
58
59
60



85x71mm (300 x 300 DPI)

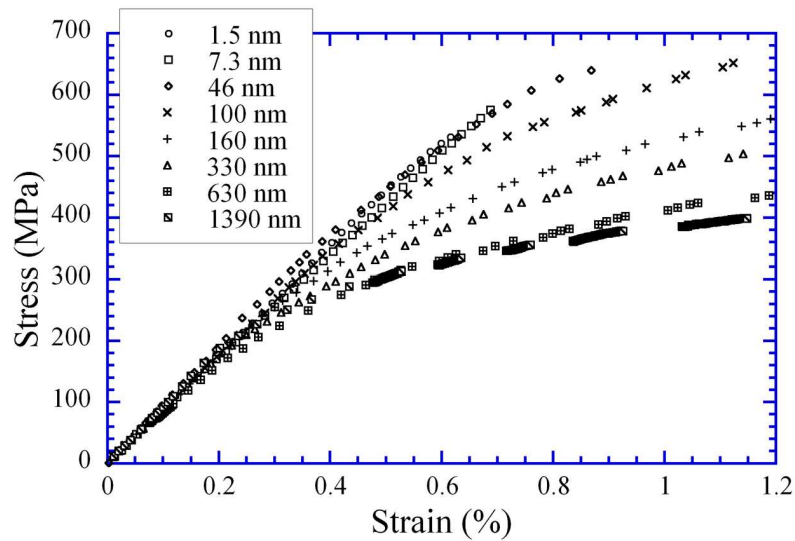
1
2
3
4
5
6
7
8
9
10
11
12
13
14
15
16
17
18
19
20
21
22
23
24
25
26
27
28
29
30
31
32
33
34
35
36
37
38
39
40
41
42
43
44
45
46
47
48
49
50
51
52
53
54
55
56
57
58
59
60



100x67mm (400 x 400 DPI)

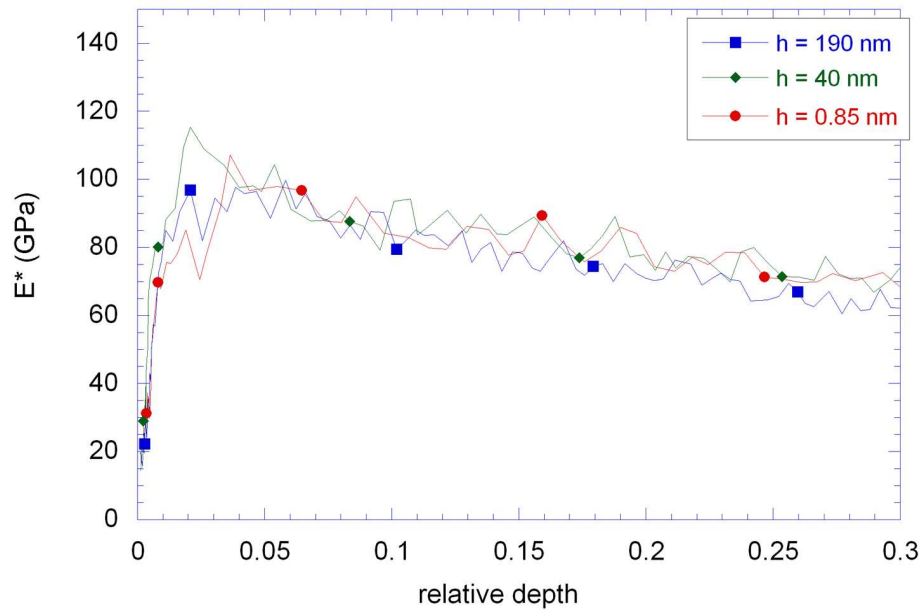
view Only

1
2
3
4
5
6
7
8
9
10
11
12
13
14
15
16
17
18
19
20
21
22
23
24
25
26
27
28
29
30
31
32
33
34
35
36
37
38
39
40
41
42
43
44
45
46
47
48
49
50
51
52
53
54
55
56
57
58
59
60



100x64mm (400 x 400 DPI)

Review Only

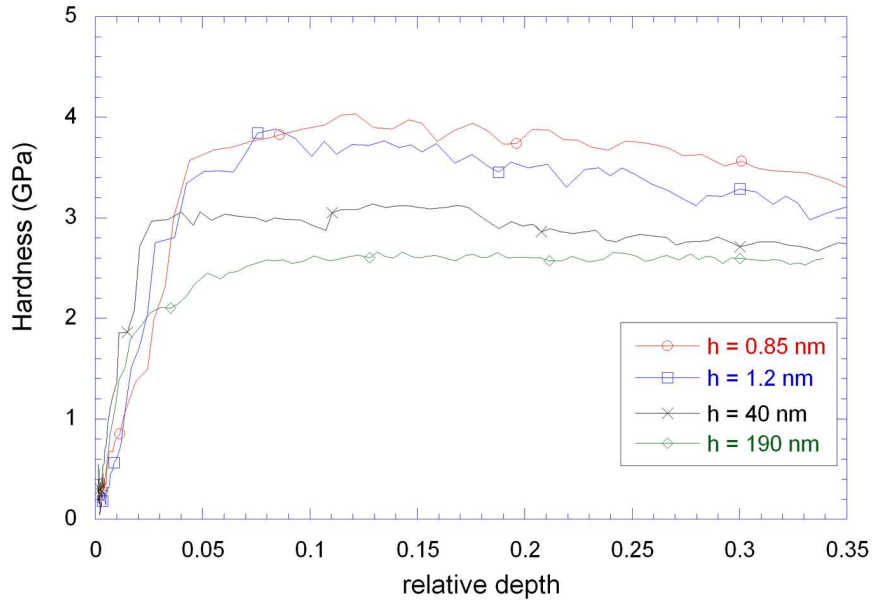


100x66mm (400 x 400 DPI)

view Only

1
2
3
4
5
6
7
8
9
10
11
12
13
14
15
16
17
18
19
20
21
22
23
24
25
26
27
28
29
30
31
32
33
34
35
36
37
38
39
40
41
42
43
44
45
46
47
48
49
50
51
52
53
54
55
56
57
58
59
60

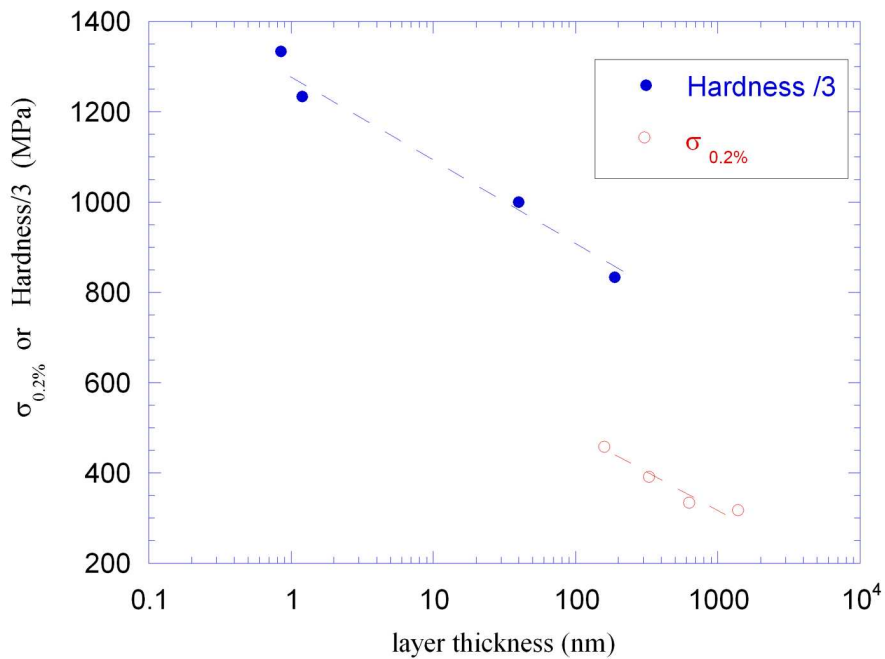
1
2
3
4
5
6
7
8
9
10
11
12
13
14
15
16
17
18
19
20
21
22
23
24
25
26
27
28
29
30
31
32
33
34
35
36
37
38
39
40
41
42
43
44
45
46
47
48
49
50
51
52
53
54
55
56
57
58
59
60



100x70mm (400 x 400 DPI)

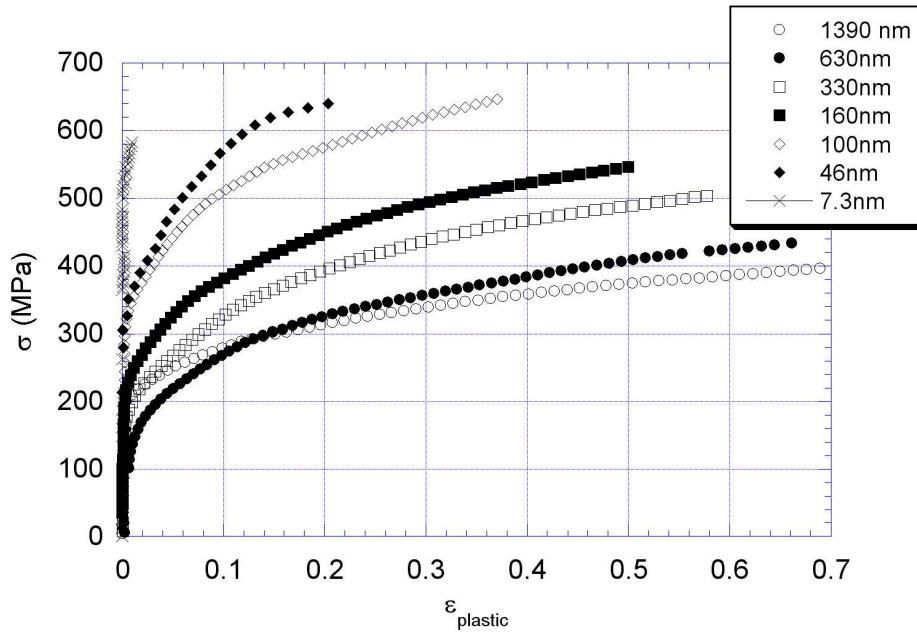
View Only

1
2
3
4
5
6
7
8
9
10
11
12
13
14
15
16
17
18
19
20
21
22
23
24
25
26
27
28
29
30
31
32
33
34
35
36
37
38
39
40
41
42
43
44
45
46
47
48
49
50
51
52
53
54
55
56
57
58
59
60



100x72mm (400 x 400 DPI)

new Only

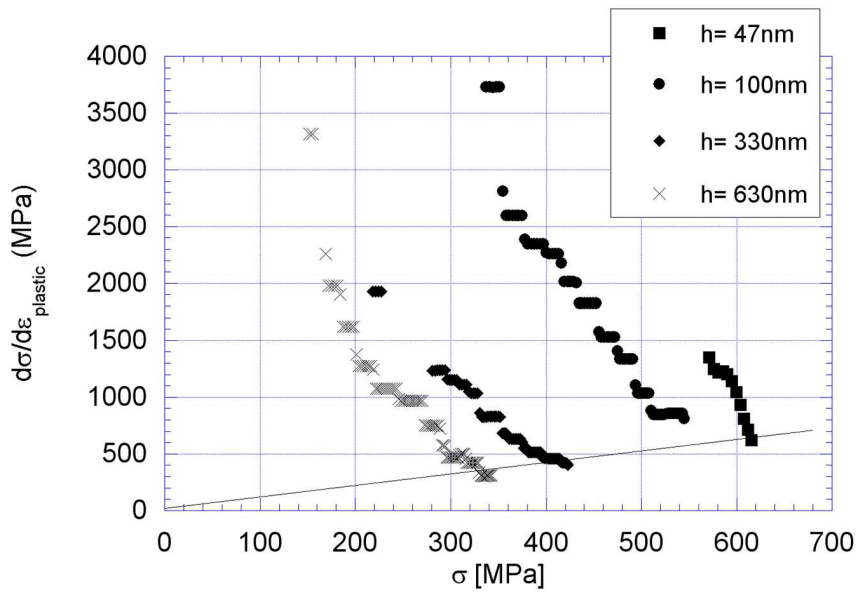


137x93mm (300 x 300 DPI)

view Only

1
2
3
4
5
6
7
8
9
10
11
12
13
14
15
16
17
18
19
20
21
22
23
24
25
26
27
28
29
30
31
32
33
34
35
36
37
38
39
40
41
42
43
44
45
46
47
48
49
50
51
52
53
54
55
56
57
58
59
60

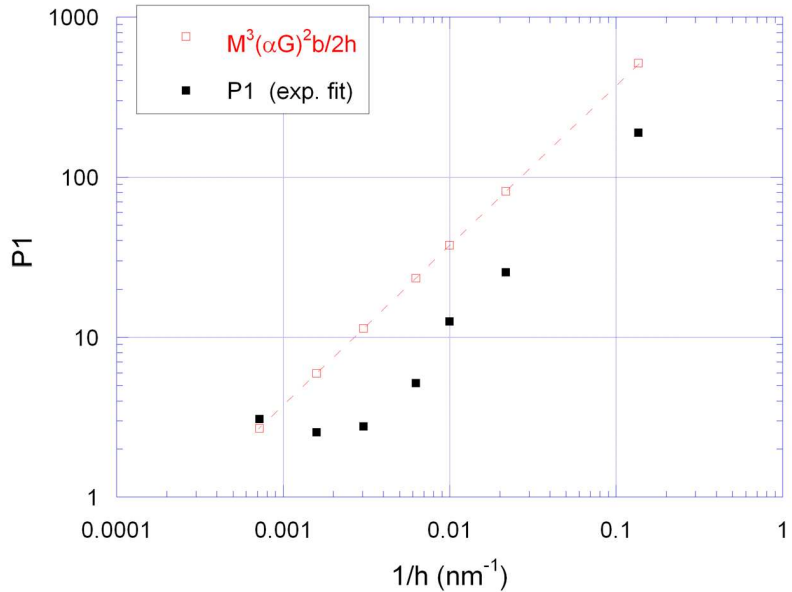
1
2
3
4
5
6
7
8
9
10
11
12
13
14
15
16
17
18
19
20
21
22
23
24
25
26
27
28
29
30
31
32
33
34
35
36
37
38
39
40
41
42
43
44
45
46
47
48
49
50
51
52
53
54
55
56
57
58
59
60



100x67mm (400 x 400 DPI)

view Only

1
2
3
4
5
6
7
8
9
10
11
12
13
14
15
16
17
18
19
20
21
22
23
24
25
26
27
28
29
30
31
32
33
34
35
36
37
38
39
40
41
42
43
44
45
46
47
48
49
50
51
52
53
54
55
56
57
58
59
60



100x71mm (400 x 400 DPI)

View Only